Absorption of subpicosecond uv laser pulses during interaction with solid targets

M. Borghesi,* A. J. Mackinnon,† R. Gaillard, and O. Willi
The Blackett Laboratory, Imperial College of Science, Medicine and Technology, London SW7 2BZ, United Kingdom

D. Riley
Department of Pure and Applied Physics, Queen's University, Belfast BT7 1NN, United Kingdom
(Received 22 February 1999; revised manuscript received 6 July 1999)

The absorption of subpicosecond uv laser pulses has been measured at intensities above 10^{17} W/cm^2. High levels of absorption were observed, up to 55% for *s* polarization and 65% for *p* polarization. The behavior with angle of incidence and polarization can be interpreted as due to a combination of resonance and collisional absorption, taking place in a plasma with a scale length of the order of a fraction of the laser wavelength. [S1063-651X(99)06011-0]

PACS number(s): 52.40.Nk, 52.25.Nr

I. INTRODUCTION

The main motivations leading to the study of the interaction of intense, short laser pulses with solid targets have been, until recently, the possibility of studying high density and temperature laboratory plasmas, and their application as a source of intense, ultrashort x-ray pulses [1]. The observation of x rays emitted from these plasma has led to a number of important results (for example, the measurement of spontaneously emitted x rays with energies exceeding 1 MeV [2]). X-ray emission measurements are closely related to absorption mechanisms, since the emission properties of plasmas depend strongly upon the degree of coupling of the laser radiation with the target. The observation of the dependence of the x-ray yield on the angle of incidence has often been related to resonance absorption processes (see, for example, Ref. [3]).

The recently proposed fast-ignitor (FI) scheme for ICF [4], however, has introduced a new and possibly more compelling reason to study the absorption of a short pulse laser in high density plasmas. In principle, suprathermal electrons, such as those required to start ignition in the FI scheme, can be generated and accelerated by an intense, short laser pulse interacting with a dense plasma [5]. In order to optimize and control the burst of high energy electrons, the mechanisms through which the energy of the short pulse laser is transferred to the plasma and into hot electrons have to be characterized and fully understood.

A number of measurements of laser energy absorption have been performed in recent years with infrared high-intensity subpicosecond laser pulses [6]. However, for applications in the fast-ignitor scheme, the use of shorter wavelength radiation (such as uv light) could be advantageous, for two reasons. First, the critical density is in this case closer to the compressed fuel core, and this will simplify all issues related to the energy transfer to the fuel. The second reason arises from $I\lambda^2$-scaling laws for the hot electron energy [7]. At the ultrahigh laser intensities required for fast ignition (10^{19}–10^{20} W/cm^2) the use of short wavelength light may be advantageous in order to limit the energy of the electrons to the MeV range. As a matter of fact, electrons with higher energies could not efficiently couple to the compressed core [4,8].

Several absorption measurements of short uv-laser pulses have been reported for intensities up to 10^{17} W/cm^2 [9–11]. In all these experiments, high levels of absorption (up to 50–60 % of the incident energy) were detected, and when the absorbed energy fraction was measured as a function of polarization and angle of incidence a different behavior for *s* polarized and *p* polarized light was observed [10]. In experiments performed at very low irradiances (for example for $I < 5\times10^{12}$ W/cm^2), the laser pulse effectively interacts with the dense cold matter (and the absorption is consistent with conventional skin depth effect) [12]. In experiments performed at higher irradiance the interpretation of the data is somehow complicated by the fact that the presence of a certain level of prepulse causes the plasma to interact with a performed plasma rather than with a solid. However, even in presence of a preplasma, the density profile will be steepened around critical by the ponderomotive pressure of the intense laser radiation [7]. It also has to be noted that ponderomotive modifications of the density profile generally produce ripples and corrugations in the critical surface [13]. In two-dimensional particle-in-cell simulations, this has been shown to lead, in the limit of ultraintense laser pulses, to the seeding of a Rayleigh-Taylor-like instability, and ultimately to hole boring [14]. The presence of such structures in the plasma can substantially affect the absorption dynamics [14–16].

All the absorption data available at intensities of about 10^{17} W/cm^2 appear to be consistent with absorption due to a combination of resonance and collisional absorption. In principle, the contribution of the two processes to the overall absorption can—to an extent—be discriminated by varying the polarization of the incident beam from *s* (laser polarization perpendicular to the plane of incidence) to *p* (laser polarization in the plane of incidence), as resonance absorption is possible only for *p* polarized light [7]. In reality, things are complicated by the fact that, due to the focusing optics, there

*Present address: Department of Pure and Applied Physics, Queen's University, Belfast BT7 1NN, United Kingdom.

†Present address: Lawrence Livermore National Laboratory, Livermore, CA.

will always be a certain degree of *p* polarized interaction, even in *s* polarization geometry or at normal incidence [17]. Irregularities of the critical (or target) surface, by reducing the distinction between *s* and *p* polarized light and virtually making impossible a well defined angle of incidence, also allow resonance absorption to occur in conditions in which nominally it should not take place [16]. As a matter of fact, at high irradiances (i.e., for $I\lambda^2 > 10^{15}\,\mathrm{W/cm^{-2}}\,\mu\mathrm{m}^2$), classical collisional absorption is expected to become progressively less important (see, for example, Ref. [7]), but the absorption levels measured experimentally seem to be systematically higher than expected from theoretical predictions [10,18]. In the experiments in which a collisionless, resonance behavior was isolated, the plasma density scale length *L* could be estimated. The values of these estimates ranged from $L/\lambda = 10$ [10] to $L/\lambda = 0.2$ [11]. These results were obtained in experiments using 12-ps and a 400-fs laser pulses respectively.

However, at larger intensities, and in presence of strong density profile steepening, other absorption mechanisms, such as the anomalous skin effect [19], vacuum heating [20] and $J \times B$ heating [14,21], are expected to become important. An anomalous behavior of the absorption was recognized in an experiment performed by Teubner *et al.* [22] using the Sprite laser at the Rutherford Appleton Laboratory, in which the absorption of a 400-fs UV laser pulse was measured at intensities exceeding $10^{18}\,\mathrm{W/cm^2}$. The higher absorption values were obtained at very large angles (75°–80°), and this behavior was attributed to absorption through anomalous skin heating in a steplike density profile.

This paper reports on experimental measurements of the absorption of subpicosecond KrF laser pulses in plasmas generated from solid targets. The absorption was measured as a function of angle and polarization, at average intensities in the range $(3-5)\times 10^{17}\,\mathrm{W/cm^2}$.

II. EXPERIMENTAL ARRANGEMENT

The experiments were performed using the Sprite [23] and the Titania [24] lasers at RAL in the chirped pulse amplified (CPA) configuration [25]. In both cases the pulse was recompressed in vacuum inside the interaction chamber, where the compression gratings were located. The Sprite laser produced KrF pulses of 500-fs duration at a wavelength of 248 nm. The short pulse was superimposed on an amplified spontaneous emission (ASE) pulse. The ASE intensity for the Sprite laser was measured in different experiments and estimated as $5\times 10^{11}\,\mathrm{W/cm^2}$ [22]. In the conditions of our experiment this corresponds to a contrast ratio of 10^6. The duration of the pulses delivered by the Titania laser was 500 fs, superimposed on an ASE pulse with an estimated contrast ratio of 10^7-10^8 [26].

The experimental arrangement is depicted in Fig. 1. In both experiments the laser pulse was focused onto target with a *f*/3.5 off axis parabola. In the Sprite measurements the targets consisted of 300-nm-thick Al layers overcoated onto a glass slide, and in the Titania measurement 250-μm-thick aluminum foils were used. In both experiments the energy on target was limited to 250 mJ by the damage threshold of the compression gratings. An image of the focal spot taken during the experimental campaign on Sprite is shown

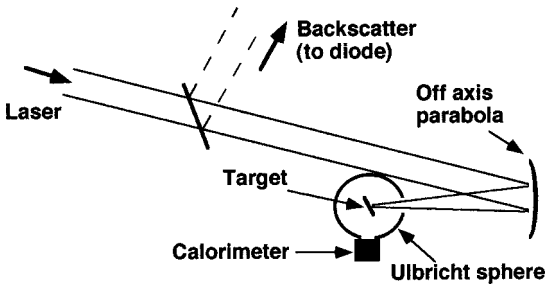

FIG. 1. Experimental setup.

in Fig. 2 (the Titania focal spot presented similar characteristics). It was obtained by imaging the focal spot at the chamber center with a *f*/2.5 lens. The average intensity on target was $(3-5)\times 10^{17}\,\mathrm{W/cm^2}$ in a focal spot with a 10–15-μm-diameter FWHM (full width at half maximum). Within the focal spot diameter, hot spots were present, with number and intensity distribution varying on a shot-to-shot basis. The absorption was measured in an indirect way, by measuring the amount of energy scattered (i.e., not absorbed) by the target. The target was placed at the center of an Ulbricht sphere [27] with a 5-cm radius. This is a plastic sphere with the inner surface painted with a diffusive, highly reflective paint (barium sulphite). Several holes are present on the surface of the sphere, to permit the access of the laser beam, the alignment of the target, and access for diagnostics. The laser radiation scattered by the target is diffusely reflected by the inner surface of the sphere. After a few reflections the laser energy is uniformly distributed over the volume of the sphere. In this way the scattered energy fraction R_S can be measured (for any scattering direction) by a surface integrating calorimeter placed at a diagnostic hole on the surface of the sphere.

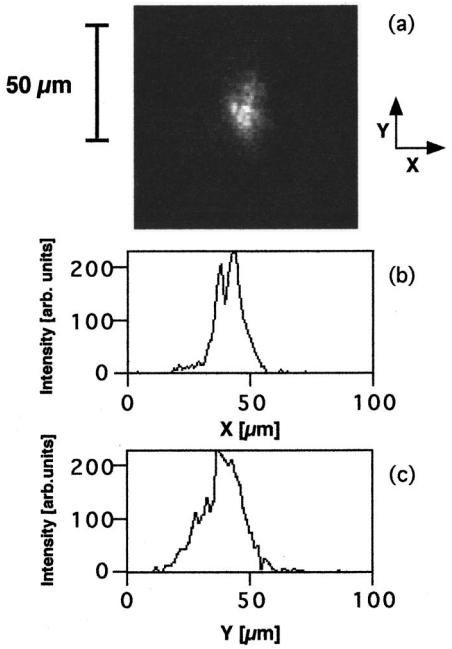

FIG. 2. (a) Image of the Sprite CPA focal spot at the chamber center, taken during an high energy shot. (b) Horizontal lineout through the center of the focal spot intensity distribution. (c) Vertical lineout through the center of the focal spot intensity distribution.

However, the radiation that is directly scattered back along the laser axis can escape from the sphere through the entrance hole, which has a 1-cm radius. The semiaperture of the acceptance cone of the entrance hole (seen from the sphere center) is $\phi_0 \approx 10°$. For small angles of incidence on target, the fraction of scattered light escaping through the entrance hole may be significant. It was therefore necessary to measure the fraction R_b of UV light backscattered into the parabola. As shown in Fig. 1, this was done with a photodiode placed outside the target chamber. The absorbed energy fraction f_A was finally estimated as $f_A = 1-(R_S+R_b)$.

The linearity of the sphere-calorimeter system and of the photodiode in the analyzed energy range was carefully checked. The Ulbricht sphere was calibrated in the following way: a large, diffusing target (coated with barium sulphite paint) was placed at the center of the sphere, and the beam was defocused to a centimeter size, so that the energy on target was below the damage threshold and all the energy incident on target was scattered inside the sphere. The calorimeter reading corresponding to 100% reflectivity (i.e., zero absorption) was obtained in these conditions.

The targets, placed at the center of the Ulbricht sphere, were mounted on a translatable rotating stage, driven by a calibrated stepper motor. The rotation angle could be determined with a precision of 2°. The laser pulse was linearly polarized in the vertical direction throughout all the measurements. However, *s* and *p* polarizations could be studied by changing the target rotation axis from vertical to horizontal. The position of the target was controlled within 10 μm with a telescope alignment system, observing the target through viewing holes on the sphere.

Since no filters were placed in front of the calorimeter and the energy measurement was time integrated, energy emitted from the plasma during and after the interaction was also collected by the calorimeter. However, from simple considerations, it can be seen that this energy is negligible if compared with the energy directly scattered from the target. In fact, an upper limit for the emission can be estimated by considering the radiation emitted by a blackbody at the temperature T_e of the plasma in the range of wavelengths that are efficiently diffused by the sphere. The intensity emitted in the range $[\lambda_1,\lambda_2]$ is obtained by integration of the Rayleigh-Jeans distribution [28]

$$M_{\Delta\lambda} = \left| -\frac{2}{3} K c \frac{T_e}{\lambda^3} \right|_{\lambda_1}^{\lambda_2},$$

where K is the Boltzmann constant. For $T_e = 1$ keV, $\lambda_1 = 0.250\,\mu$m, and $\lambda_2 = 2.5\,\mu$m, one obtains $M_{\Delta l} \approx 6 \times 10^8$ W/cm^2. Taking reasonable values as a plasma radius $r = 50\,\mu$m and an average emission duration $\Delta t = 100$ ps (the emission from the plasma will last for much longer, but the temperature of the plasma will quickly decrease as the plasma expands), one can estimate the energy emitted in the range $[\lambda_1,\lambda_2]$ as $E_{\Delta\lambda} \approx M_{\Delta\lambda} \pi r^2 \Delta t \approx 4 \times 10^{-6}$ J. This value is much smaller than the typical scattered energies measured during the experiments (in the range $2-20 \times 10^{-2}$ J).

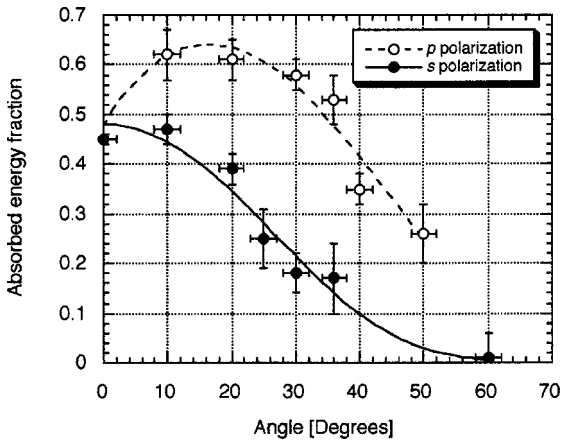

FIG. 3. Angular dependence of the absorbed energy fraction during the interaction of the 400-fs Sprite KrF pulse with Al targets. The lines are the best fits, using the functions described in the text.

III. MEASUREMENTS, ANALYSIS, AND DISCUSSION

In both experiments, two different sets of measurements were performed, using *s* and *p* polarized light. The results of these two series of measurements are shown in Figs. 3 and 4. Every point is the average of at least three different measurements.

The measurements show an absorption level for normal incidence as high as 50–60%, and a different angular dependence of the absorption for *s* and *p* polarized light. While the absorption for *s* polarized light decreases from the normal incidence value as the angle of incidence increases, the absorption level for *p* polarized light reaches a broad maximum for $\theta = 10°-20°$ in the Sprite measurements, and about $\theta \approx 30°$ in the Titania measurements.

In a first approximation the data can be analyzed under the assumption that all the absorption at normal incidence and for *s* polarized light is due to collisional absorption, while the absorption for *p* polarized light is due to a combination of resonance and collisional absorption. However, as pointed out earlier, the mixing of polarization due to focusing can result in a component of resonance absorption even in the *s* polarized case and at normal incidence. For example, in Ref. [11] this was shown to be a significant effect. This

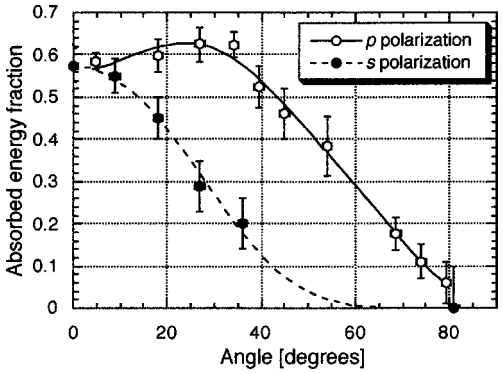

FIG. 4. Angular dependence of the absorbed energy fraction during the interaction of the 500-fs Titania KrF pulse with Al targets. The lines are the best fits, using the functions described in the text.

was related to the fact that the effective angle of incidence due to focusing was a significant fraction of the angle at which maximum resonance absorption occurred. Also, as mentioned in Sec. I, laser-induced deformations of the critical surface can lead to some degree of resonance absorption even for light that is not *p* polarized. Thus some care must be taken in assigning the absorption for normal incidence and *s* polarization to collisional absorption only, and, while it will be ignored in this first approximation, the importance of polarization mixing due to focusing and critical surface deformations will be estimated later in the text.

The angular dependence for *s* polarization follows qualitatively the expected behavior for collisional absorption. The laser intensity is reduced on the way up to critical, and on the way back after the reflection, by a factor $e^{-\delta}$, where δ is a decreasing function of the angle of incidence θ. An analytical solution can be obtained in the conditions to which the WKB approximation applies [7].

The angular behavior of the absorption for *p* polarized light is consistent with a combination of resonance and collisional absorption. In fact, at low angles, collisional absorption, which does not depend on polarization, contributes in keeping the absorption level high, while a resonance process peaking at larger incidence must be responsible for the absorption at larger angles, when the collisional process becomes less important. In order to isolate the contribution of resonance absorption in the data for *p* polarized light, a description of the collisional absorption fraction is required. For this purpose, the *s* polarization data have been fitted with a function resembling the WKB expressions for collisional absorption, as given for example in Ref. [7], i.e., $f_s(\theta)=1-\exp[-A\cos^n(\theta)]$, where A and n are left as free parameters. The parameter n depends, in the WKB theory treatment, on the type of plasma density profile assumed in the calculations. A function of this kind was found to describe the data reasonably well, as visible in Figs. 3 and 4, and the best fit was obtained for $n\approx 7$. However this value does not correspond to any known density profile, and it is used only to describe empirically the data.

As mentioned above, for *s* polarized light the energy is absorbed through bremsstrahlung absorption as the pulse propagates up the density gradient to the turning point, and on the way back after reflection. If, as the fit suggests, the laser intensity for *s* polarized light is reduced by a factor $\exp[-\delta(\theta)]$ after two-way propagation in the plasma, the reduction in intensity for *p* polarized light incident at the angle θ can be estimated as $[(1-f_r(\theta)]\times\exp[-\delta(\theta)]$, where f_r is the function describing resonance absorption.

The absorbed energy fraction after two-way propagation for *p* polarized light is therefore given by $f_p(\theta)=1-[1-f_r(\theta)][1-f_s(\theta)]$. The *p* polarization data have been fitted with the above function. $f_s(q)$ is the best fit for the *s* polarization data, and $f_r(\theta)$ a polynomial function of the type $f_r(\theta)=\Sigma_{i=1}^{n} c_i\theta^i$, with c_i a free parameter. The best fit obtained using the function f_p is also shown in Figs. 3 and 4, and describes reasonably well the experimental data. From the fit, the functions f_r (shown in Fig. 5), describing resonance absorption in the two experiments, are obtained.

The peak of the resonance profile is at about 27° for the Sprite measurements, and at about 35° for the Titania measurements. From the angle of maximum absorption, an approximate value of the plasma scale length L close to the critical density can be deduced. According to Denisov's theory [7], the resonance absorption reaches a maximum when $\tau=(\omega L/c)^{1/3}\sin(\theta)\approx 0.8$. This gives, for $\theta_{\max}=27°$, $L\approx 0.9\lambda\approx 0.2\,\mu$m, and, for $\theta_{\max}=35°$, $L\approx 0.4\lambda\approx 0.1\,\mu$m. However, the use of the above formula, obtained in a WKB treatment, is strictly valid only for density profiles with $L/\lambda\gg 1$.

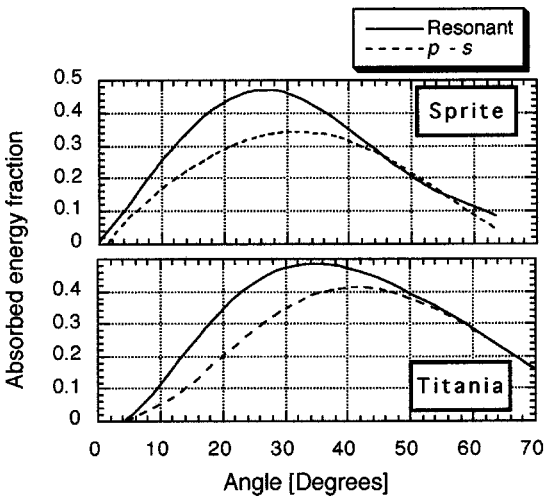

FIG. 5. Solid line: resonance absorption profile inferred from the data of Figs. 3 and 4 (following the method explained in the text). Dashed line: Simple difference between the *p* polarization and *s* polarization absorption profiles.

An alternative procedure to infer the density scale length was given in Ref. [29]. In this reference the Helmholtz wave equation was numerically solved, and the difference between the absorbed energy fraction for *p* and *s* polarized light was plotted as a function of the angle of incidence. The angle $\theta^*_{\max}$ at which the difference between *p* and *s* absorption peaks depends unambiguously on the density scalelength L for a wide range of scale lengths. Therefore, the plasma scale length can be deduced from the value of $\theta^*_{\max}$. In our case (see Fig. 5) $\theta^*_{\max}\approx 30°$ for the Sprite results and $\theta^*_{\max}\approx 40°$ for the Titania measurements. Following Fig. 1 of Ref. [29], one obtains $L\approx 0.6\lambda\approx 0.15\,\mu$m for $\theta^*_{\max}\approx 30°$ and $L\approx 0.2\lambda\approx 0.05\,\mu$m for $\theta^*_{\max}\approx 40°$. From all these estimates the measurements seem to indicate that the plasma scale length was of the order of a fraction of the wavelength. It was shorter for the Titania experiment, and this is consistent with a lower prepulse level.

Also, the scalelength seems to be short enough that resonance absorption due to focusing is not very important in these experiments. This can be estimated, as in Ref. [10], by using the Denisov model of resonance absorption [7], which gives the absorbed energy fraction f_A as $f_A=\phi^2(\tau)/2$, where $\phi(\tau)\approx 2.3\tau\exp(-2\tau^3/3)$, and τ is the parameter defined previously. The maximum value of absorption occurs for $\tau\sim 0.8$. From these formulas, a value of τ can be estimated for values of θ away from peak absorption, and consequently the resonance absorption due to focusing for nominally normal incidence can also be evaluated. With the focusing optics of the experiments, and by assuming a Gaussian profile in the near field, an average over the energy in the beam gives a weighted average angle of incidence of $\sim 5°$ for nominally

normal incidence. Using the model outlined above, it can be estimated that, for the Titania data, if the peak resonance absorption is at 40°, then, at normal incidence, the resonance absorption present is only ~3%. As the peak absorption is ~55% at normal incidence, this effect does not seem to be too important. For the Sprite data, from a peak at 30° the resonance absorption at normal incidence can be determined to be ~5%, again much less than the actual observed absorption.

Another effect, thus far neglected, which can raise the absorption level at normal incidence or for *s* polarized light is the onset of irregularities at the critical density surface. The effect of these ripples or ''bubbles'' will be to reduce the distinction between *s* and *p* polarized light and to smooth out the angular dependence of the absorption, as, on the scale of the surface deformations, there will not be a well defined angle of incidence or a well defined polarization. In the experiments reported here such ripples could be seeded by nonuniformities of the target surface, or, via the ponderomotive pressure of the hot spots present in the focal spot. A simple estimate of the relative importance of ponderomotive and thermal pressure can be obtained by considering the ratio between the quiver velocity v_{os} and the thermal velocity v_{th} [7], i.e., $v_{os}/v_{th} \sim (I/10^{17}\,\mathrm{W/cm^2})^{0.5}/[T_e\,(\mathrm{keV})]^{0.5}$ for $\lambda = 0.25\,\mu$m. As an example, according to this simple estimate, for $I = 5\times10^{17}\,\mathrm{W/cm^2}$, ponderomotive and thermal pressure will be of the same order if $T_e \approx 5$ keV. Indication that ponderomotive effects play a role in compressing the plasma in the intensity and pulselength regimes of the experiment reported here has been obtained both experimentally [30] and computationally [31].

If, following Refs. [14] and [16], one supposes the ponderomotive pressure to be stronger than the thermal pressure, the depth of the hole ponderomotively bored by the laser focal spot (or by hot spots in the laser intensity profile) into an overdense plasma of density n_e can be roughly estimated, as $a \approx 2\times10^{-9}(c\tau_L)[(n_c/2n_e)(Z/A)(I\lambda^2)]^{0.5}$ where τ_L is the pulse duration, m_e the electron mass, m_i the ion mass, Z the charge state, and cgs units are used. For parameters of the order of the experimental ones ($\tau_L = 400$ fs, $I = 5\times10^{17}\,\mathrm{W/cm^2}$, and choosing, for example, $n_e = 10\,n_c$), the depth of such a hole would be of the order of 0.1 μm. A small change in the angle of incidence (about 2°) would be introduced by such a deformation, if one takes the 10-μm FWHM focal spot diameter as its transverse size. The effect could be larger if the deformation is produced by a hot spot, as the local intensity could be higher and the radial extent of the deformation smaller.

This effect is expected to be more pronounced for an incidence close to normal, as the laser pulse can propagate closer to the critical density and its ponderomotive force can act more efficiently on the critical surface. It should be pointed out that, even supposing that no collisional absorption was present, some of the observed angular features could, in principle, be qualitatively explained by this effect alone. If one assumes that the main absorption mechanism is resonance (peaking at an angle θ_{max}), deformations of the critical surface, being stronger for angles near zero incidence, would cause the *p* polarization absorption to stay high even for $\theta < \theta_{max}$, since they would allow interaction at angles close to θ_{max} to take place even for normal or near-normal incidence. The same effect would tend to eliminate the differences between *s* and *p* polarization at small angles, allowing *p* polarized interaction even for *s* polarized light. As the strength of the deformation decreases with the angle of incidence, the amount of resonance absorption taking place for *s* polarized light would also decrease. As a matter of fact, in the Titania data, it can be seen that for angles up to 10–15° there is little difference between the absorption for *s* and *p* polarized data, while in the Sprite data set, the difference at 10° is already quite large. This could be explained by the fact that, due to the lower prepulse level and, consequently, to the steeper density profile, the Titania pulse's ponderomotive force interacted more efficiently with the critical density, leading to more important deformations.

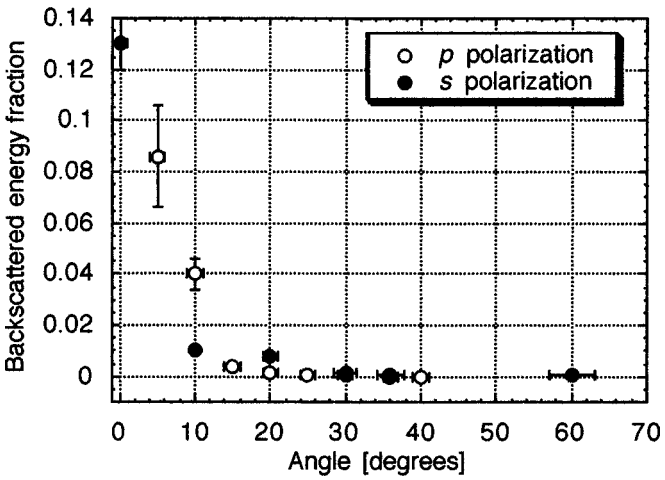

FIG. 6. Backscattered energy fraction measured as a function of the angle of incidence using the Sprite laser.

As previously observed, it is somehow difficult at present to estimate the real importance of this effect and to determine, for example, how much of the absorption at normal incidence is due to collisional absorption or to resonance absorption in a structured plasma. This has to be taken as a present limit of these studies. However, some additional indication can be inferred by observing the angular distribution of the backscattered radiation.

The level of the radiation scattered from the target back through the entrance hole—$b(\theta)$—is shown in Fig. 6 as a function of the angle of incidence. Only the results from the Sprite campaign are shown here. The measurements obtained with Titania present similar characteristics, but with some scatter of the backscattered level in the measurements taken at large angles, possibly due to roughness of the target surface.

As can be seen in Fig. 6, a considerable level of backscattered radiation was measured only for incidence close to 0°. The maximum level detected (at 0°) was 13% of the incident energy. Since the amount of the total energy scattered from the target was 55% of the incident radiation, only about 25% of the light diffused from the target is intercepted by the entrance hole. This seems to imply that the radiation is scattered into a relatively large cone. This could be due to refractive effects in the focal region [10,18], or to the onset of deformations of the critical surface [16].

If we assume for simplicity that, in a plane perpendicular to the direction of specular reflection, the distribution of en-

ergy is cylindrically symmetric and has a Gaussian radial dependence of the type $I=I_0\exp[-2r^2/r_0^2]$, where r_0 is the beam radius, a rough estimate of the width of the scattering cone can be obtained. This approach would indicate, for example, that the energy is scattered by the target into a $f/1$ cone ($f/1$ being the divergence of the $1/e^2$ surface). This corresponds to an half-aperture of about 27°, much larger than the half aperture of the focusing cone, which is of the order of 8°. Due to the finite aperture of the scattered light, the backscatter level falls as the incidence angle is increased and the energy intercepted by the entrance hole becomes marginal. Further, if the angular spread is to some extent caused by deformations of the critical density, the strength of the deformations (and the angular aperture of the scattered radiation) should decrease as the angle of incidence increases. This would make the radiation intercepted by the entrance hole fall even more rapidly.

As an example, the effect of the angular spread introduced by target deformations can be estimated following Ref. [16]. By assuming a deformation depth a, treating the laser reflection from the deformed critical surface as from a spherical mirror, and taking the transverse size of the deformation r, it can be shown that the additional angular spread $\Delta\alpha$ (half-aperture) introduced by the reflection is approximately given (in radiants) by $4a/r$. As an example one could get an angular spread as that observed in the experiment ($\Delta\alpha \approx 19°$), taking $a=0.13\,\mu$m (of the order of the deformation calculated previously) and $r=1.5\,\mu$m (of the order of the radius of an hot spot). Under these conditions, if one neglects the focusing effects, radiation with nominal normal incidence would be incident with a range of angle varying from 0 to $2a/r$ radiants. By assuming a Gaussian intensity distribution in the hot spot, an energy-weighted average angle can be evaluated, giving $\langle\alpha\rangle\approx a/r(\approx 4°-5°)$. Again, this indicates that the change in angle of incidence is perhaps too small to have on its own an effect comparable to the absorption levels measured at normal incidence. However, it cannot be excluded that the combined effect of focusing optics and target deformation could be responsible for a sizable fraction of the light absorbed at normal incidence.

Finally, the fact that the level of backscatter is very small (below 1%) for angles larger than 30° also indicates that the amount of backscattered light due to parametric instabilities is not significant. This seems to confirm that the scale length of the preplasma was not long.

IV. COMPARISON WITH OTHER RESULTS

As is clear from Sec. III the measurements performed on Sprite can be, in principle, satisfactorily explained with a combination of collisional and resonance absorption, taking place in a plasma with a scale length of the order of a fraction of the laser wavelength. This is consistent with other measurements previously performed at similar (or slightly lower) irradiances, as for example those reported by Teubner and co-workers [11,18] using a 400-fs KrF laser.

However, measurements performed by Teubner and coworkers using the Sprite laser at RAL, [22] in similar experimental conditions, gave different results, as already mentioned in Sec. I. The angular dependence was measured for p polarized light at the highest irradiance available. A peak laser intensity of $2.5\times10^{18}\,\mathrm{W/cm^2}$ was inferred in these conditions, and the absorption was seen to increase as the angle of incidence was increased, reaching the maximum (75%) at 80°. This behavior was explained as due to the anomalous skin effect [19]. The absorption was also measured as a function of the laser intensity at the fixed incidence angle of 67°. In particular, an absorption of about 50% was measured at $10^{17}\,\mathrm{W/cm^2}$ for p polarized light. No difference was observed at this angle between the absorption measured for s and p polarized light.

On the basis of the experimental data, it is difficult to explain the discrepancy between the measurements reported here and the measurements reported in Ref. [22]. The peak intensity inferred in Ref. [22] is considerably higher than the one reported in the present paper, however this may depend to some extent on the way the intensity on target is defined. As a matter of fact, Teubner and co-workers estimated the intensity considering that 30% of the energy is contained in an area with a diameter of 3 μm, while the remaining 70% is distributed within a 15–20-μm diameter. Nevertheless, parameters as the focusability of the beam or the main-to-prepulse contrast ratio may have been optimized more efficiently in Ref. [22] than in the experiment here reported. A better quality focal spot (leading to a more effective ponderomotive force) and the minimization of a preplasma would both lead to interaction with a steeper density gradient, and the absorption mechanisms involved could change significantly.

Recently, results obtained at higher irradiance [16] showed an angular behavior not dissimilar to the one observed in the Sprite and Titania experiments reported here. This experiment was performed at the Limeil P102 facility, France. In this case 15% of the 5-J energy on target was contained in a 5-μm central spot, giving an intensity of up to $10^{19}\,\mathrm{W/cm^2}$ locally, while the rest of the energy was distributed over a 40-μm diameter focal spot, resulting in an average intensity on target of about $10^{18}\,\mathrm{W/cm^2}$. However, since the wavelength was 0.527 μm, the effective average irradiance was higher than in the KrF experiments discussed above. The absorption for s polarized light was seen to decrease monotonically as the angle increased, while the absorption for p polarized light peaked at 25°, with a maximum value of 45%. Due to the very high main-to-prepulse contrast ratio (10^{12}), the absorption was expected to peak at large angles, as observed in Ref. [22]. The behavior observed was in this case completely different. Although it seems difficult to isolate the contribution of the various absorption mechanisms, it was inferred that modifications in the surface morphology played an important role in determining the absorption features. This assumption was correlated to the onset at high intensities of diffusion (rather than reflection) from the target. Qualitatively (although not quantitatively) the angular behavior observed in Ref. [16] is similar to the one observed in the experiments reported in this paper. However, due to the higher irradiance and contrast ratio in Feurer *et al.*'s experiment, it is reasonable to assume that the effect of ponderomotive deformation was larger in their case.

Finally, harmonic emission efficiency measurements recently performed on the Rutherford KrF laser system [32] were consistent with the absorption behavior observed in our experiment. The efficiency of third harmonic emission was

measured, as a function of the angle of incidence, during the interaction of 1-ps, *p* polarized KrF pulses, focused at an intensity of about $10^{18}\,W/cm^2$ on solid targets. An extremely strong dependence of the emission on the angle of incidence was observed, with peak conversion occurring at about 30°. In other words, the data indicate a more efficient coupling of the laser with the near-critical plasma around this angle, as consistent with the resonance behavior inferred by the measurements reported in this paper.

V. CONCLUSIONS

Absorption measurements were performed using the KrF lasers Sprite and Titania, that delivered pulses with duration $\tau \approx 400-500\,fs$ and average intensities up to $5\times10^{17}\,W/cm^2$, with a main to prepulse contrast ratio of 10^6 and 10^7-10^8, respectively. The pulse was focused onto Al targets, and the energy absorbed during the interaction was measured, varying incidence angles and polarization, by using an Ulbricht sphere and a calorimeter. As observed in other measurements performed in similar interaction conditions, high levels of absorption were detected, both for *s* and *p* polarized light. An energy fraction up to 65% of the incident energy was absorbed (55% for normal incidence). The behavior with angle of incidence and polarization can be interpreted as due to a combination of collisional and resonance absorption. By assuming that all the absorption at normal incidence and for *s* polarized light is due to collisional processes, a plasma density scale length of the order of a fraction of the laser wavelength is inferred from the resonance peak. However, and although difficult to quantify, the contribution of residual resonance absorption processes to the laser absorption at normal incidence or for *s* polarized light cannot be excluded. In fact, laser induced deformations of the critical surface can make resonance absorption possible even in conditions in which it should nominally not take place. The fact that the cone of the light scattered from the target was larger than the cone of the focusing optics is indeed consistent with the presence of structures in the critical surface. Although estimates based on the inferred backscatter cone seem to indicate that the residual resonance absorption due to this effect alone should not be too important, nevertheless the combined effect of laser induced ripples and focusing effects could cause a significant level of resonance absorption for nominally non-*p* polarized light. The comparison of these results with other absorption measurements obtained in the same regime of intensities shows that the mechanisms of the laser absorption in this regime are not still sufficiently clear. Indeed, a very different behavior has been observed in an experiment performed on the same laser system, in which no resonance, but an angular dependence of the absorption consistent with anomalous skin effect was observed. One has to conclude that the absorption features in these interaction regimes depend strongly on parameters that may vary from experiment to experiment, as for example the prepulse level or the beam quality. As a matter of fact, the variability of the results is a general characteristic of the absorption experiments that have been performed at intensities exceeding $10^{17}\,W/cm^2$. Indeed, theoretical and computational studies have pointed out the absorption mechanisms that are expected to be important in high intensity interactions. However, it seems that a full understanding of the relative importance of these mechanisms, and of the way they apply to realistic situations, can be achieved only at the cost of performing a large number of experiments, and of controlling the experimental parameters as strictly as possible.

ACKNOWLEDGMENTS

The authors would like to thank the staff of the Rutherford Appleton Laboratory, and in particular the personnel of the Sprite/Titania lasers, for the help and assistance received during the experiments, and to acknowledge useful discussions with S. M. Viana. This work was funded by EPSRC/MoD grants.

[1] M. M. Murnane, H. C. Kapteyn, M. D. Rosen, and R. W. Falcone, Science **251**, 797 (1993).

[2] J. D. Kmetec, C. L. Gordon, J. J. Macklin, B. E. Lemoff, S. G. Brown, and S. E. Harris, Phys. Rev. Lett. **68**, 1527 (1992).

[3] L. A. Gizzi, D. Giulietti, A. Giulietti, P. Audebert, S. Bastiani, J. P. Geindre, and A. Mysyrowicz, Phys. Rev. Lett. **76**, 2278 (1996).

[4] M. Tabak, J. Hammer, M. Glinsky, W. L. Kruer, S. C. Wilks, and A. B. Langdon, Phys. Plasmas **1**, 1626 (1994).

[5] P. Gibbon and A. R. Bell, Phys. Rev. Lett. **68**, 1535 (1992).

[6] M. Chaker, J. C. Kieffer, J. P. Matte, H. Pepin, P. Audebert, P. Maine, D. Strickland, P. Bado, and G. Mourou, Phys. Fluids B **3**, 167 (1991); D. D. Meyerhofer, H. Chan, A. Delettrez, B. Soom, S. Uchida, and B. Yaakobi, *ibid.* **5**, 2584 (1993); D. F. Price, R. M. More, R. S. Walling, G. Guethlein, R. L. Sheperd, R. E. Stewart, and W. E. White, Phys. Rev. Lett. **75**, 252 (1995); M. Schnurer, M. P. Kalashnikov, P. V. Nickles, Th. Schlegel, W. Sandner, N. Demchenko, R. Nolte, and P. Ambrosi, Phys. Plasmas **2**, 3106 (1995).

[7] W. L. Kruer, *The Physics of Laser Plasma Interaction*, (Addison-Wesley, New York, 1998).

[8] C. Deutsch, H. Furukawa, K. Mima, M. Murakami, and K. Nishihara, Phys. Rev. Lett. **77**, 2483 (1996).

[9] R. Fedosejevs, R. Ottmann, R. Sigel, G. Kühnle, S. Satzmari, and F. P. Schäfer, Phys. Rev. Lett. **64**, 1250 (1990); R. Sauerbrey, J. Fure, S. P. LeBlanc, B. Wan Wonterghem, U. Teubner, and F. P. Schafer, Phys. Plasmas **1**, 1635 (1994).

[10] D. Riley, L. A. Gizzi, A. J. Mackinnon, S. M. Viana, and O. Willi, Phys. Rev. E **48**, 4855 (1993).

[11] U. Teubner, J. Bergmann, B. wan Wonterghem, F. P. Schäfer, and R. Sauerbrey, Phys. Rev. Lett. **70**, 794 (1993).

[12] J. C. Kieffer, P. Audebert, M. Chaker, H. Pepin, T. W. Johnston, P. Maine, D. Meyerhofer, and J. Delettrez, Phys. Rev. Lett. **62**, 760 (1989).

[13] E. J. Valeo and K. Estabrook, Phys. Rev. Lett. **34**, 1008 (1975); D. W. Forslund, J. M. Kindel, K. Lee, and E. L. Lindman, Phys. Rev. Lett. **34**, 193 (1975); K. Estabrook, Phys. Fluids **19**, 1733 (1976).

[14] S. C. Wilks, W. L. Kruer, M. Tabak, and A. B. Langdon, Phys.

Rev. Lett. **69**, 1383 (1992); S. C. Wilks, Phys. Fluids B **5**, 2603 (1993).
[15] H. Ruhl, A. Macchi, P. Mulser, F. Cornolti, and S. Hain, Phys. Rev. Lett. **82**, 2095 (1999).
[16] T. Feurer, W. Theobald, R. Sauerbrey, I. Uschmann, D. Altenbernd, U. Teubner, P. Gibbon, E. Forster, G. Malka, and J. L. Miquel, Phys. Rev. E **56**, 4608 (1997).
[17] A. Boivin and E. Wolf, Phys. Rev. **138**, B1561 (1965); R. P. Godwin, Appl. Opt. **33**, 1063 (1994).
[18] U. Teubner, P. Gibbon, E. Forster, F. Fallies, P. Audebert, J. P. Geindre, and J. C. Gauthier, Phys. Plasmas **3**, 2679 (1996).
[19] E. S. Weibel, Phys. Fluids **10**, 741 (1967); A. A. Andreev, E. G. Gamalii, V. N. Novikov, A. N. Semakhin, and V. T. Tikhonchuk, Zh. Eksp. Teor. Fiz. **101**, 1808 (1992) [Sov. Phys. JETP **74**, 963 (1992)].
[20] F. Brunel, Phys. Rev. Lett. **59**, 52 (1987); Phys. Fluids **31**, 2714 (1988).
[21] W. L. Kruer and K. Estabrook, Phys. Fluids **28**, 430 (1985).
[22] U. Teubner, I. Uschmann, P. Gibbon, D. Altenbernd, E. Forster, T. Feurer, W. Theobald, R. Sauerbrey, G. Hirst, M. H. Key, J. Lister, and D. Neely, Phys. Rev. E **54**, 4167 (1996).
[23] J. M. D. Lister, E. J. Divall, S. W. Downes, C. B. Edwards, G. J. Hirst, C. J. Hooker, M. H. Key, I. N. Ross, M. J. Shaw, and W. T. Toner, J. Mod. Opt. **41**, 1203 (1994).
[24] E. J. Divall, C. B. Edwards, G. J. Hirst, C. J. Hooker, A. K. Kidd, J. M. D. Lister, R. Mathumo, I. N. Ross, M. J. Shaw, W. T. Toner, A. P. Visser, and B. E. Wyborn, J. Mod. Opt. **43**, 1025 (1996).
[25] D. Strickland and G. Mourou, Opt. Commun. **56**, 219 (1985); P. Maine, D. Strickland, P. Bado, M. Pessot, and G. Mourou, IEEE J. Quantum Electron. **QE24**, 398 (1988).
[26] J. D. Lister (private communication).
[27] R. P. Godwin, R. Sachsenmaier, and R. Sigel, Phys. Rev. Lett. **39**, 1198 (1977).
[28] J. McCartney, *Absorption and Emission by Atmospheric Gases—The Physical Processes* (Wiley, New York, 1975).
[29] O. L. Landen, D. G. Stearns, and E. M. Campbell, Phys. Rev. Lett. **63**, 1475 (1989).
[30] X. Liu and D. Umstadter, Phys. Rev. Lett. **69**, 1935 (1992); O. Peyrusse, M. Busquet, J. C. Kieffer, Z. Jiang, and C. Y. Coté, *ibid.* **75**, 3862 (1995).
[31] U. Teubner, P. Gibbon, E. Forster, F. Fallies, P. Audebert, J. P. Geindre, and J. C. Gauthier, Phys. Plasmas **3**, 2679 (1996).
[32] D. M. Chambers, P. A. Norreys, A. E. Dangor, R. S. Marjoribanks, S. Moustaizhs, D. Neely, S. G. Preston, J. S. Wark, I. Watts, and M. Zepf, Opt. Commun. **148**, 289 (1998).